Crystallization Kinetics of Pure and Binary Melts

D. J. KIRWAN and R. L. PIGFORD
University of Delaware, Newark, Delaware

An absolute rate theory based on a plausible model of the activated state, was developed for the interfacial kinetics of crystal growth from the melt. Except for liquid metals the theory predicts the growth rates of pure materials within about an order of magnitude. A microinterferometric technique was employed to observe liquid compositions near the faces of crystals growing from binary melts. For the simple eutectic system composed of salol and thymol, the theory represents the composition and temperature dependence of the growth rate.

The preparation of pure materials by crystallization from solution is a common separation technique in the process industries. There is interest in crystallization from the melt because of its importance to operations associated with the electronics industry, such as single crystal preparation and zone refining. In addition, there is considerable attention being devoted to the development of continuous fractional solidification processes for the separation of organic materials (*1, 2*).

The growth of a crystal from a binary melt, as in fractional solidification, involves heat and mass transfer in two bulk phases and a kinetic process at the solid-liquid interface. Although the transport processes that occur in the bulk phases can be fairly well described, the interfacial kinetic process is not well characterized at present. The rational design of melt crystallizers requires that both the magnitude of this so-called "interfacial resistance" and its proper rate expression be known.

The purpose of this work was to investigate the interfacial crystallization kinetics of pure and binary melts, that is, the relationships between the rates of freezing of species in a liquid mixture and the departure of the interface conditions from equilibrium. That the interface is not at equilibrium follows immediately from the fact that one phase is growing at a finite rate at the expense of the other. This is not to say that in many cases, due to the relative magnitudes of the interfacial and bulk phase resistances, the departure from interfacial equilibrium may not be immeasurably small.

For approximately seventy years investigators have been reporting the dependence of the freezing rates of pure liquids on the applied undercooling. Much of this work is summarized by Van Hook (*3*). In a recent book, Chalmers (*4*) has discussed the solidification of metals and alloys. Cahn, Hillig, and Sears (*5*) have reviewed the theoretical and experimental information on the interfacial kinetics for the growth of crystals from pure melts.

It is now recognized that the growth rate of a crystal from the melt is strongly dependent upon the structure of the solid-liquid interface. Growth on close packed faces of a crystal is presumed to occur by the lateral motion of steps across the crystal face. The source of these steps may be either two-dimensional nuclei for perfect faces or self-perpetuating defects such as screw dislocations intersecting the crystal surface (*5*). According to the theory of Cahn (*6*) if the departure from equilibrium becomes large enough, the interface becomes molecularly rough and growth occurs by random incorporation of molecules onto the surface rather than attachment only at steps that sweep across the crystal face. Jackson (*7*) has presented a theory for predicting whether an interface in contact with the melt will be rough or smooth.

Hillig and Turnbull (*8*) considered the growth of a crystal from a pure melt when a screw dislocation mechanism prevails. They assumed that the rate of addition of molecules to an advancing step occurs by a monomolecular transport process. This rate was computed by using the concepts of absolute rate theory. In reasonable agreement with the experimental evidence available at the time, their theory predicted a quadratic dependence of growth velocity on the undercooling at the interface for small values of the undercooling. In the absence of better information they assumed that the activated state for crystallization was similar to that for viscous flow or self-diffusion in the liquid.

Theoretical or experimental studies of the crystallization kinetics of binary melts are few in number. Chalmers et al. (*4*) developed a kinetic theory of alloy solidification based upon an activated state concept, but the theory contained accommodation coefficients and geometric parameters for the solid-liquid interface which are not readily obtained. In the design of crystallizers the interfacial rate expression for a solute crystallizing from solution is usually assumed to be similar to that of a simple reversible chemical reaction (*9, 10*). In the zone refining literature, the equilibrium distribution coefficient is commonly used to relate the concentration of solute in the solid to that in the liquid at the interface, even though the finite rate of growth may cause significant departures from equilibrium.

In the following sections, a theory for the crystallization rates of species from a multicomponent melt will be developed, and experiments will be described in which crystallization rates in a simple eutectic system were observed under measured interfacial conditions.

THEORY

In this section an interfacial rate expression will be derived for the crystallization of each species of a mixed crystal from the melt. Ideally, crystallization rate expres-

---

D. J. Kirwan is with Monsanto Company, St. Louis, Missouri and R. L. Pigford is with the University of California, Berkeley, California.

sions would be developed from kinetic theories of the liquid and solid states; however, such theories are not sufficiently developed at present to yield any significant results for condensed phases. For condensed phases the absolute rate theory of Eyring et al. (*11*) offers perhaps the only theoretical framework for the prediction of rate processes. At best only order of magnitude estimates might be expected from the absolute rate theory applied to crystal growth kinetics.

In general the growth rate of a crystal is governed by the rate of addition of molecules to growth sites on the surface and by the density of such sites on the crystal face. Analogous to the developments of Hillig and Turnbull (*8*) and Clifton (*12*) for pure components, the net crystallization flux of species *i* may be written in absolute rate theory terms as

$$N_i = f\lambda\rho^s[k_i^f y_i - k_i^r x_i] \qquad (1)$$

where the forward and reverse rate constants are given by the usual absolute rate expressions

$$k_i^f = \kappa\,(kT/h)\Gamma_i \exp\,[-\,\Delta\mu_i^{\neq f}/RT] \qquad (2a)$$

$$k_i^r = \kappa\,(kT/h)\gamma_i \exp\,[(\Delta\mu_i^o - \Delta\mu_i^{\neq f})/RT] \qquad (2b)$$

The factor, *f*, the surface step density, is the fraction of the crystal face available for attachment. The interface advances a distance, λ, when a monomolecular layer is added to the solid. The standard free energy of activation for the freezing of component *i* is $\Delta\mu_i^{\neq f}$ while $\Delta\mu_i^o$ is the standard (pure component) free energy change when *i* transforms from the liquid to the solid state at the interface temperature, *T*.

$$\Delta\mu_i^o = \int_{T_i}^{T} \frac{\partial\Delta\mu_i^o}{\partial T}\,dT \sim -\,\Delta S_i(T_i - T) + \Delta c_{pi}[T_i - T + T\ln(T/T_i)] \qquad (3)$$

An interfacial transport coefficient for motion across the liquid-solid interface, having the same units as a diffusion coefficient, may be defined by the equation

$$D_i = \lambda^2\kappa(kT/h)\Gamma_i \exp\,(-\,\Delta\mu_i^{\neq f}/RT) \qquad (4)$$

The crystallization rate can then be put in the familiar form of a rate coefficient times a driving force. Thus

$$N_i = f\rho^s(D_i/\lambda)\,[y_i - (\gamma_i x_i/\Gamma_i)\exp(\mu\Delta_i^o/RT)] \qquad (5)$$

Equation (5) can also be expressed in terms of the existing chemical potential difference of species *i* across the interface, $\Delta\mu_i = \mu_i^l - \mu_i^s$.

$$N_i = f\rho^s(D_i/\lambda)y_i[1 - \exp(-\,\Delta\mu_i/RT)] \qquad (6)$$

If equilibrium exists between solid and liquid at the interface temperature, the chemical potentials in the two phases are equal and the crystallization rate is zero, as it must be at equilibrium.

Surface Step Density

The density of growth sites, or steps, on the surface is dependent upon the character of the solid-liquid interface. For a molecularly rough interface (5) all sites on the crystal are available for attachment and *f* has a value of unity.

For a perfect crystal face a two-dimensional nucleation process would be required to provide growth sites. However, most real crystals have surface defects and grow bounded by close packed faces. As first noted by Frank (*13, 14*), a screw dislocation intersecting a crystal face provides a self-perpetuating step source for growth on close packed faces. If such a mechanism is correct, growth should occur in the form of a spiral or pyramid on the face of the crystal, as sketched in Figure 1. Growth spirals have been observed on crystals grown from vapor, from solution, and from melt thus providing graphic support for Frank's hypothesis (*3*).

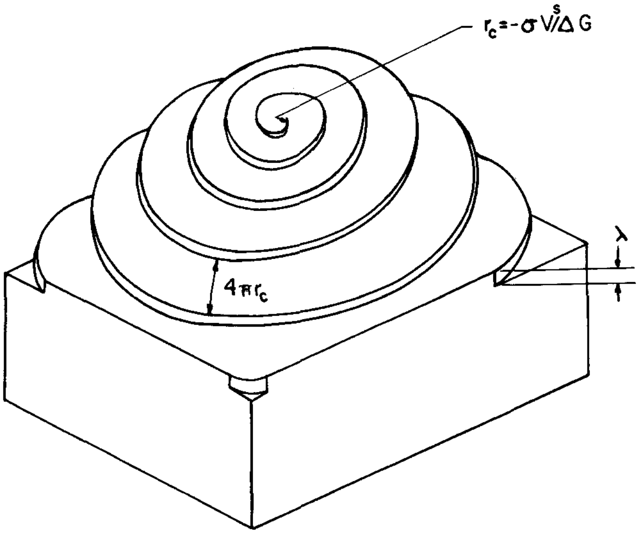

Fig. 1. Growth spiral.

Frank approximated the growth spiral by an Archimedes spiral. The step density is then given in terms of the intermolecular spacing and the radius of a critical size two-dimensional nucleus, which can be expressed in terms of the interfacial free energy per unit of surface and the free energy change when one mole of solid is formed from the liquid:

$$f = \lambda/4\pi r_c = -\,\lambda\Delta G/4\pi\sigma V^s \qquad (7)$$

If the difference in heat capacities of the solid and liquid is neglected, then for a pure melt, $\Delta G = \Delta\mu_i^o \sim -\,\Delta S\Delta T$. The step density is proportional to the undercooling at the interface

$$f = (\lambda\Delta S/4\pi\sigma V^s)\Delta T \qquad (8)$$

Corresponding expressions for other types of dislocations acting as step sources have not as yet been developed.

Interfacial Transport Coefficient

To calculate a value for D_i, the transport coefficient for motion across the liquid-solid interface, a configuration for the activated state must be assumed. As previously mentioned, Hillig and Turnbull (*8*) identified the crystallization activated state with that for viscous flow in the liquid. The absolute rate theory expression for the viscosity of a liquid (*11*) is

$$\eta = (1/\kappa)\,(h/\lambda^3)\exp(\Delta G_v^{\neq}/RT) \qquad (9)$$

For the viscous flow model the crystallization transport coefficient would then be expressed in terms of the liquid viscosity, where the slightly different definitions of λ, the intermolecular spacing, have been ignored:

$$D_i = (kT/\lambda\eta)\Gamma_i \qquad (10)$$

The predicted values of crystallization rates of pure materials based on this equation were in reasonable agreement with experiment in some cases, but were in error by as much as four orders of magnitude in others, for example, phosphorus, (*8*).

There is some evidence that the activation energy for crystallization is smaller than that for viscous flow (*8, 12, 15*). It would seem reasonable that crystallization rates might be more accurately predicted by postulating a more realistic activated state. To do this we compare the condition of a molecule activated for viscous flow to that of a molecule activated to incorporate itself into a crystal.

The activation free energy of a process can be written *formally in* terms of an activation enthalpy and an activation entropy, such as

$$\Delta G^{\ddagger} = \Delta H^{\ddagger} - T\Delta S^{\ddagger} \tag{11}$$

It will be useful to estimate these terms separately.

Enthalpy of Activation

The activation enthalpy for viscous flow is sometimes considered to be the sum of the enthalpy, $\Delta H_v^{\ddagger j}$, required to activate a molecule for flow and the enthalpy, $\Delta H_v^{\ddagger h}$, to make a nearby hole in the liquid into which the molecule may jump (*14, 16, 17*). Therefore

$$\Delta H_v^{\ddagger} = \Delta H_v^{\ddagger j} + \Delta H_v^{\ddagger h} \tag{12}$$

In principle, the activation enthalpy for jumping can be obtained from the variation of viscosity with temperature at constant volume and the activation enthalpy for hole formation can be obtained by difference, knowing the variation of viscosity with temperature at constant pressure. In practice, however, the necessary experimental data are rarely available.

Let us compare the activation enthalpy required for crystallization to that for viscous flow. Consider a possible crystallization activated state for a molecule in the melt adjacent to a step or growth site on a crystal face. When it comes from the liquid, a molecule must possess the activation enthalpy to jump to a growth site on the solid surface, just as in viscous flow. However, because of the presence of the solid surface and the step on the surface, the activation enthalpy associated with hole formation is probably not required. The hole or growth site is always present at the step on the surface. Furthermore, the presence of the crystal surface probably results in more free volume in the liquid adjacent to the surface, analogous to the increased void space in a packed bed of solid particles near the walls of the container (*18*). This local rarefaction of the liquid density near the surface will probably act to lower the activation enthalpy for jumping. This effect would be difficult to estimate, so for a first approximation we neglect it and estimate the activation enthalpy for crystallization as equal to the activation enthalpy for jumping in viscous flow:

$$\Delta H_i^{\ddagger} = \Delta H_v^{\ddagger j} \tag{13}$$

For binary mixtures the partial molar enthalpy of activation for crystallization of component i is required. As for pure components, this can be approximated by the partial molar activation enthalpy for jumping in viscous flow. Whitaker and Pigford (*16*) discuss how the partial molar activation enthalpy of i for jumping might be obtained from the total partial molar activation enthalpy of i in the liquid mixture. The simplest assumption, corresponding to a thermodynamically ideal system, would be to take the partial molar activation enthalpy in the mixture equal to the pure component value. Because of the uncertainties in the estimation of the activation enthalpy for jumping from the total activation enthalpy, a detailed analysis of the effect of composition is probably not justified.

Entropy of Activation

Although a crystallizing molecule encounters a lower enthalpy barrier than a molecule in viscous flow, unless it is spherically symmetric, it encounters a greater entropy barrier. While a molecule in viscous flow can be oriented in almost any direction, a crystallizing molecule must be oriented so as to fit into the crystal lattice. Otherwise, it will be rejected at the growth site. Orientation entropy effects would seem to be a reasonable explanation for the much slower growth rates of complex organic molecules compared to simple liquids and liquid metals.

The activation entropy for crystallization may be estimated as the activation entropy for viscous flow plus the entropy decrease associated with a molecule being oriented as rigidly as in the solid. This orientation entropy is approximated as the entropy of fusion minus R, since simple spherical molecules and atoms, for which orientation effects are absent, normally have entropies of fusion of about 2 e.u., corresponding to the gain of the "communal entropy" of the liquid (*19*). The activation entropy for crystallization is then written as

$$\Delta S^{\ddagger} = \Delta S_v^{\ddagger} - (\Delta S - R) \tag{14}$$

where ΔS is the pure component entropy of fusion.

For mixtures the partial molar activation entropy is required just as for the enthalpy. This can be estimated from Equation (14) by using the viscous flow activation entropy of the mixture and the pure component entropy of fusion. Again, the estimate of the crystallization activation entropy is so approximate that a detailed analysis of composition effects is not justified.

The activation free energy for crystallization is then estimated from Equations (13) and (14) as

$$\Delta\mu_i^{\ddagger f} = \Delta H_{i,v}^{\ddagger j} - T[\Delta S_v^{\ddagger} - (\Delta S_i - R)] \tag{15}$$

From Equations (5) and (15) the interfacial transport coefficient may be written as

$$D_i = \lambda^2\kappa(kT/h)\Gamma_i \exp[(-\Delta H_{i,v}^{\ddagger j}/RT) + (\Delta S_v^{\ddagger} - (\Delta S_i - \mathrm{R}))/R] \tag{16}$$

When the viscosity of the melt is used to evaluate $\Delta S_v^{\ddagger}$ and $\Delta H_{i,v}^{\ddagger j}$ Equation (16) becomes

$$D_i = [(kT/\lambda\eta)\Gamma_i]\exp(\Delta H_{i,v}^{\ddagger h}/RT)\exp(1 - \Delta S_i/R) \tag{17}$$

The expression in brackets in Equation (17) represents the viscous flow model estimate of the transport coefficient. The additional terms in Equation (17), involving the activation enthalpy for hole formation and the entropy of fusion minus R, have counteracting effects. This partially explains why the viscous flow model predicts reasonable values of the rate coefficient in some cases. The activation enthalpy for crystallization is less than that for viscous flow but the entropy barrier is larger so that the effects compensate despite the unrealistic assumption that the activated states for viscous flow and crystallization are similar.

For nonassociating, spherical molecules, for example, phosphorus, P_4, the entropy of fusion is small and the hole formation activation enthalpy is a large percentage of the total viscous activation enthalpy (*16, 17*). The contributions of these terms will therefore be larger than one and the predicted crystallization rate larger than that obtained from the viscous flow model. For large complex molecules, ΔS, is large and the correction to the viscous flow model prediction may be either greater or less than unity depending upon the hole formation enthalpy.

EXPERIMENTAL PROCEDURE

A microinterferometric method was selected to permit the observation of concentrations and concentration gradients in the melt near the growing face of a crystal. The interferometric technique had previously been used to observe concentration fields about crystals growing from aqueous solution at room temperature (*20 to 22*) and to measure liquid-liquid diffusion coefficients (*23,24*). Details of the interferometric equipment used by the authors can be found elsewhere (*25*). Only a brief summary of the principles of the method and the experimental technique will be given here.

The basis of the interferometric method can be explained with reference to the schematic drawing in Figure 2. Crystallization occurs in a thin film of liquid in an optical wedge formed by two partly aluminized glass slides illuminated by a source of parallel, monochromatic light. The wedge is placed on a microscope hot stage for temperature control and is observed with a microscope and associated photographic equipment. A helium-neon gas laser was used as the light source because its high intensity allowed photographs to be taken with short exposure times and it was also a convenient source of parallel monochromatic light. If the material in the wedge is of uniform refractive index, a pattern of straight parallel fringes appears in the eyepiece of the microscope.

Consider the crystallization of a binary melt in the wedge. Since the composition of the solid differs from that of the liquid from which it is frozen, the composition of the liquid at the interface will differ from that of the original liquid far from the interface. The refractive index will therefore vary as the interface is approached which will result in a corresponding curvature of the interference fringes near the interface. An interference fringe is a locus of equal optical paths, that is, the product of refractive index and wedge thickness is a constant. A typical interferogram is shown in Figure 3. A knowledge of the wedge thickness and the refractive index-composition relationship of the liquid permits the composition and composition gradients about the growing crystal to be obtained from measurements of the fringe shift.

The experiments were carried out by bringing the stage to a temperature below the liquidus temperature of the melt to be crystallized. A portion of the melt was introduced into the wedge and allowed to equilibrate. A small seed crystal touched to the edge of the wedge initiated crystallization. The growing crystal and its associated fringe pattern were observed by time lapse photography through the microscope using a 16mm. movie camera and a timer. The growth velocity was obtained from the known time between frames and the magnification of the microscope and camera. Liquid composition was calculated from the fringe pattern and the known original composition. The temperature of the melt was obtained from a copper-constantan thermocouple placed in a well near the bottom plate of the wedge. The thermocouple readings had previously been calibrated against those of a 0.003 in. diam. thermocouple placed within the wedge during a dummy run. The wedge thickness at each point of interest was calculated from the distance to the apex of the wedge and the wedge angle.

Owing to the latent heat released at the interface, the interface temperature tended to rise above that of the surroundings. This temperature rise also caused a fringe curvature just as a composition change did. The magnitude of this temperature rise was evaluated by crystallizing pure materials in the wedge since all fringe curvature could then be attributed to a temperature gradient. The temperature rise never exceeded 2.5°C. for growth velocities in the range of 4 to 17×10^{-3}cm/sec. This information was used to correct the observed interfacial undercoolings and concentrations when correlating the crystallization rate data.

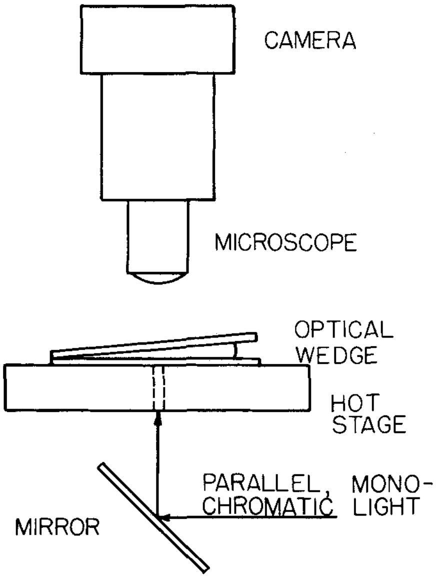

Fig. 2. Microinterferometric apparatus.

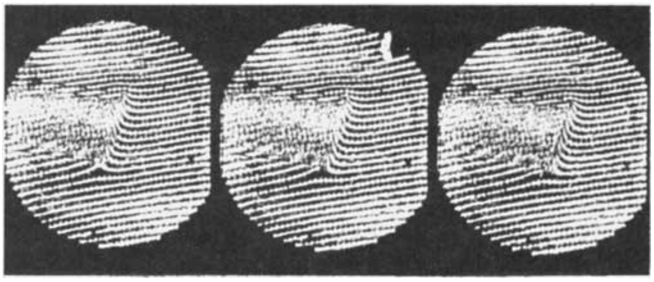

Fig. 3. Interferogram of thymol crystal growing from binary melt × 50.

Crystallization rates of salol-thymol mixtures were observed as well as the freezing rates of the pure materials. Salol (phenyl salicylate) and thymol (3-p-cymenol) form a simple eutecic system whose phase diagram is given by Timmermanns (*26*). At low undercoolings the crystals grew with well defined faces, but as the undercooling increased the growth front became irregular and polycrystalline. On the basis of other investigators' work (*27,28*) and the appearance of the crystals, it is believed that it was on close packed faces such as the (100) and (111) that growth rates were observed. Considerable refinement in the experiemental technique would be required to observe and compare the growth rates of different crystallographic faces under measured interfacial conditions.

Some experiments were also performed with the isomorphous system: trans-stibene-bibenzyl. However, the melts did not undercool readily and the growth velocities were rapid, making the experiments difficult to carry out. In addition, a satisfactory method of measuring the instantaneous composition of the solid freezing out could not be developed, owing to the thinness of the crystal plates.

The interferometric method provides a means for directly observing interfacial liquid compositions during crystallization. In general, the technique works best for systems that subcool readily, crystallize relatively slowly (<0.1cm/sec.), and have crystal habits consisting of plates or prisms rather than needle-like forms.

RESULTS

Pure Component Crystallization Rates

In this section crystal growth rates predicted by the absolute rate theory expression developed here are compared with experimental values of the growth rates of pure materials available in the literature or obtained by the authors. In Table 1 are listed the various physical and thermodynamic properties used in the calculation of the crystal growth rates. The interfacial free energies per unit area were calculated from Turnbull's correlation (*29*). The activation enthalpy for viscosity was evaluated at the melting point of the material by differentiation of viscosity data obtained from the literature. The intermolecular spacing, λ, was taken as the cube root of the molecular volume of the solid.

In order to compute the interfacial transport coefficient, the jumping and hole formation activation enthalpies for viscous flow must be known. Literature values are available for only two of the substances studied, water and benzene (*16*). The activation enthalpies could have been computed if the variation of viscosity with temperature at constant volume as well as at constant pressure was known. This information was not available for the substances of interest. However, some general rules relating these activation enthalpies to the total activation enthalpy for viscosity can be formulated from values of other substances

TABLE 1. PHYSICAL PROPERTIES OF SELECTED PURE MATERIALS

Substance	λ, Å	T_i, °K.	ΔH,* cal./mole	ΔS,* cal./mole °K.	$\sigma \times 10^7$, cal./sq. cm.	η, centipoise	$\Delta H^{\neq}_v$, cal./mole	$\Delta H^{\neq h}_v$, cal./mole
water	3.1	273.2	1,480	5.3	7.7	1.8	4,900	980
glycerine	4.9	291.1	4,440	15.2	9.1	1,700	15,900	3,180
salol	6.6	314.8	4,670	14.8	5.5	10.0	7,860	1,570
tin	3.1	504.0	1,715	3.4	15.2	2	1,280	1,150
phosphorous	4.9	317.5	600	1.89	1.25	1.8	2,680	2,420
thymol	7.1	321.8	4,160	12.8	5.5	6.0	8,140	1,630
benzene	5.2	278.6	2,360	8.5	4.4	0.95	2,680	1,740
gallium	2.7	302.9	1,330	4.4	9.2	1.9	912	820
bromine	4.3	265.9	2,560	9.7	6.6	1.4	1,840	1,660
nickel	2.2	1728.0	4,340	2.5	80.5	4.0	1,000	900
stilbene	6.4	397.0	7,080	17.8	8.7	1.0	3,270	2,120

* Fusion.

in the literature (*16, 17*). Nonassociating liquids have larger values of $\Delta H_v^{\neq h}$ than $\Delta H_v^{\neq j}$. Typically, $\Delta H_v^{\neq h}$ is about 70 to 90% of the total activation enthalpy for viscous flow. For associated (that is, hydrogen bonded) liquids the jumping activation enthalpy is the larger quantity, presumably because of the increased difficulty in breaking hydrogen bonds when a molecule is moved through the liquid as compared to disturbing the liquid structure when forming a hole. $\Delta H_v^{\neq h}$ is about 30% of $\Delta H_v^{\neq}$ for aliphatic alcohols except for methanol, where it is about 50% of the total (*17*). The only value available for hydrogen bonded aromatic compounds is for aniline (*30*) where $\Delta H_v^{\neq j} =$ 4,300 cal./mole and $\Delta H_v^{\neq} =$ 4,700 cal./mole. For water, Whitaker and Pigford (*16*) obtained a value near zero for the hole formation enthalpy.

Based on the above literature values, the activation enthalpies for hole formation for the substances listed in Table 1 were obtained by using the following rules:

1. For the simple, nonassociated liquids, phosphorus, tin, gallium, bromine, and nickel; $\Delta H_v^{\neq h}$, the hole formation activation enthalpy was assumed to be 90% of $\Delta H_v^{\neq}$. For these substances, $\Delta H_v^{\neq}$ is relatively small so that a different choice for $\Delta H_v^{\neq h}$, for example, 0.70 $\Delta H_v^{\neq}$, would have changed the predicted velocities by only 10 to 20%.
2. For the more complex nonassociated substances, benzene and stilbene; $\Delta H^{\neq h}$ was taken as 0.65 $\Delta H^{\neq}$ in agreement with the value for benzene given by Whitaker (*16*).
3. As previously mentioned, $\Delta H_v^{\neq h}$ is about 30% of $\Delta H_v^{\neq}$ for aliphatic alcohols while it is only about 10% for the hydrogen bonded aromatic, aniline. As an approximation, $\Delta H_v^{\neq h}$, for the associated aromatic compounds, salol and thymol, was taken as 0.2 $\Delta H_v^{\neq}$.
4. Finally, $\Delta H_v^{\neq h}$ for the strongly hydrogen bonded materials, water and glycerine, should be less than that of the simple alcohols but a value of zero seems to be too extreme. $\Delta H_v^{\neq h}$ for these substances was also assumed to be 0.2 $\Delta H_v^{\neq}$.

To predict the pure component crystallization rates, it is necessary to know the nature of the solid-liquid interface in order to obtain the growth site density, *f*. With the possible exceptions of bromine, gallium, and stilbene, the substances listed in Table 1 have all been found to exhibit an approximately quadratic dependence of growth rate on undercooling, indicating a screw dislocation mechanism (*5, 8, 31* to *33*). The data obtained for stilbene by the present authors for small undercoolings are not accurate enough to determine the dependence of growth rate upon undercooling of the interface. Clifton (*12*) measured the growth rates of bromine and gallium in capillary tubes and found them to be approximately linear for undercoolings greater than 1 deg. No correction was made for the temperature rise at the interface, so that the true dependence of the rate on interface undercooling is unknown but would vary more strongly than linearly. This is particularly significant for bromine which had a freezing velocity of about 0.2 cm./sec. at 2 deg. of observed undercooling. The gallium data were linear to approximately 20 deg. undercooling and had a freezing velocity about an order of magnitude lower than that of bromine.

Figure 4 presents a comparison of the measured and predicted values of the rate coefficient (velocity/driving force) evaluated at the melting point for the substances listed in Table 1. For bromine and gallium, the experimental rate coefficient was simply taken as the freezing velocity at an observed undercooling of 1 deg. The value of the rate coefficient, *m*, was predicted, assuming a screw dislocation mechanism prevails, by combination of Equations (5), (8), and (16) evaluated for a pure material at low undercoolings.

$$m \equiv V/(\Delta T)^2$$
$$= [(\Delta S)^2 k/4\pi\sigma R V^s \lambda \eta] \exp [(\Delta H_v^{\neq h}/RT) + (1 - \Delta S_i/R)] \quad (18)$$

The expression in the first bracket represents the prediction of the rate coefficient based on the viscous flow model of the activated state as proposed by Hillig and Turnbull. This prediction is included in Figure 4 for comparison.

With the exception of bromine the predictions which used the proposed crystallization activated state are an improvement over the viscous flow activated state of Hillig and Turnbull. With the exceptions of tin and benzene, the rate coefficient is predicted within an order of magnitude of the measured value. If Jackson's criterion (*7*) is used, tin would be predicted to have a rough interface rather than obeying a lateral growth law. However, the careful measurements of Kramer and Tiller (*32*), at very small undercoolings, clearly show a quadratic dependence upon the undercooling at the interface; this is in agreement with a lateral growth mechanism.

Two experimental values are shown for the growth rates of ice that correspond to the growth direction which is parallel, or perpendicular, to the basal plane. The growth rate is about an order of magnitude smaller for growth perpendicular to the basal plane (*5*).

Although the proposed model is an improvement over the viscous flow results, it should be recognized that the assumptions and approximations of the model are still unrefined. As long as rate processes are described in terms of macroscopic models rather than molecular theories, the relevance of the model to physical reality is open to ques-

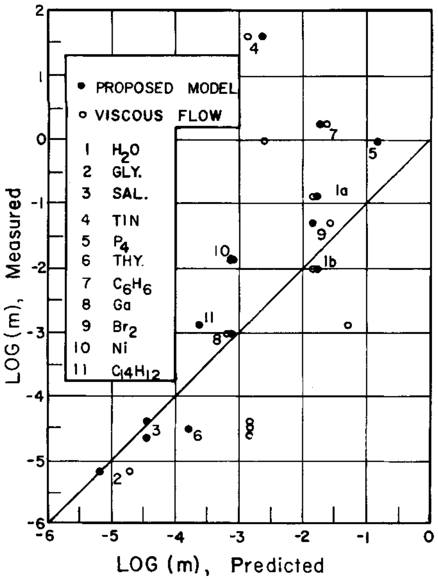

Fig. 4. Crystallization rate coefficients of pure materials.

tion. On the other hand, until molecular-kinetic theories are further advanced, the macroscopic theories do provide a convenient theoretical framework and moderate predictive abilities.

Growth From Binary Melts

For crystal growth in a binary system that exhibits no solid solubility in which a screw dislocation mechanism is assumed to prevail, the crystallization velocity is

$$V_i = N_i/\rho^s = [(\lambda\Delta\mu_i/4\pi\sigma V^s)(D_i/\lambda)] \cdot y_i\,[1-\exp(-\Delta\mu_i/RT)] \quad (19)$$

The chemical potential difference across the interface may be expressed in terms of the subcooling from the liquidus curve. Therefore we obtain

$$\Delta\mu_i = [\Delta H_i^o/T^* - \Delta c_{pi}(1-T/T^*) - R\ln\Gamma_i y_i][T^*-T] \quad (20)$$

where T^* is the liquidus temperature of a melt of mole fraction y_1. For moderate undercoolings the expression in brackets is nearly equal to the pure component entropy of fusion.

If the transport coefficient in the liquid mixture is assumed to be approximately that of the pure melt, that is, the ideal solution assumption, then

$$D_i = (kT/\lambda\eta_i^o)\exp(\Delta H_v^{\ddagger h}/RT)\exp(1-\Delta S_i^o/R) \quad (17)$$

The crystallization velocity of a pure component from a binary melt can be written as

$$V_i/y_i = [\Delta S_i^o\, kT/4\pi\sigma\eta_i^o V^s]\Delta T \cdot [1-\exp(-\Delta S_i^o\,\Delta T/RT)] \cdot \exp(\Delta H_v^{\ddagger h}/RT)\exp(1-\Delta S_i^o/R) \quad (21)$$

Equation (21) predicts that the crystallization velocity divided by the interfacial liquid mole fraction depends only upon the undercooling of the interfacial liquid and is independent of the melt composition, provided the transport coefficient is approximately independent of composition.

Analogous to a pure melt, the term, $1-\exp(-\Delta S_i^o\Delta T/RT)$, in Equation (21) may be approximated by its Taylor series expansion

$$1 - 1 + \Delta S_i^o\Delta T/RT - 1/2(\Delta S_i^o\Delta T/RT)^2 + \ldots$$

For low undercoolings this term reduces to $\Delta S_i^o\Delta T/RT$. Hence the crystallization velocity divided by the interfacial liquid composition is predicted to be proportional to the square of the undercooling from the liquidus temperature as the undercooling becomes very small. The region of validity of this approximation of course depends upon the magnitudes of the entropy of fusion and the undercooling.

The crystallization velocities of salol and thymol are plotted in Figures 5 and 6 in the manner suggested by Equation (21). Here the complete exponential term is used, rather than the Taylor series approximation, since the entropy of fusion of these materials is about 15 cal./mole-°K. It is shown (*25*) that salol and thymol mixtures form nearly ideal solutions so that the neglect of composition effects on the transport coefficient is probably justified.

For salol crystallization the theoretical curve is in reasonable agreement with the data, especially in view of the 1 to 2 deg. uncertainty in the measured interface temperature. The combined data of Pollatschek (*34*) and of Neumann and Micus (*35*) for the crystallization velocity of pure salol is also shown in Figure 5 (the dashed curve) and is in good agreement with the theoretical curve. Because of the much stronger variation of the growth velocity with undercooling than with melt composition and the scatter in the data at a given undercooling, a test of the linear dependence of velocity on interfacial liquid composition could not be made. However, the velocity divided by the liquid mole fraction gave a smoother correlation than the velocity alone. The interfacial liquid mole fractions ranged from 0.75 to 1.0 for the data shown. The vertical lines through some of the data points represent the spread of measured velocities when more than one value was obtained at very nearly the same interface conditions; the data point itself represents the average of the velocities.

The theoretical prediction of the crystallization rate for thymol freezing from the melt is approximately an order of magnitude too large, although the dependence upon the square of the supercooling is about right. Again the data do not show a trend with composition, in agreement with Equation (21), but it is not possible to test the linear dependence of crystallization velocity on interfacial liquid composition. The liquid mole fraction varied from 0.63 to 1.0 in this case. The horizontal lines through some of the data points represent the variation in undercooling along

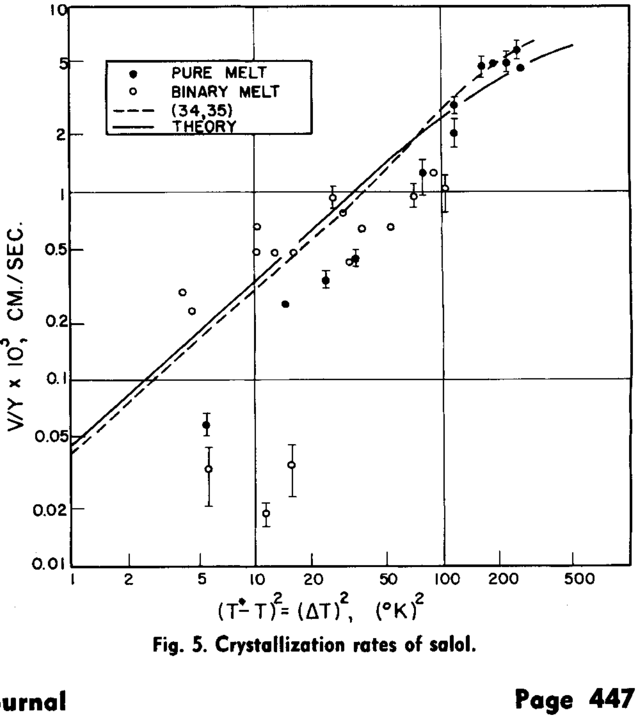

Fig. 5. Crystallization rates of salol.

the crystal face whose velocity was measured. The minimum undercooling always occurred in the center of the face.

The theoretical equations assume that the growth mechanism is a lateral one due to screw dislocations present on the crystal face. The calculation of f, the step density, assumes that growth spirals are present on the growing crystal face. Evidence in support of this mechanism for salol and thymol has been obtained by Amelinckx (*36*, *37*) who observed growth spirals on the faces of thymol and salol which were growing from the melt and from various solutions. Also the data in Figures 5 and 6 are in reasonable agreement with a quadratic dependence on undercooling at small values of ΔT.

Solid Solutions

Because of the moderate success in the use of the absolute rate theory expression to predict crystallization rates in pure melts and binary systems that exhibit no solid solubility, it is of interest to see what information can be obtained from this approach for systems that form solid solutions. Of particular interest is the prediction of the composition of solid freezing from a liquid mixture under nonequilibrium conditions.

The composition of solid freezing from a binary liquid is expressed in terms of the individual crystallization fluxes:

$$x_A = 1/(1 + N_B/N_A) \tag{22}$$

If the molar fluxes are written using the absolute rate theory developed here, the solid composition is

$$x_A = \cfrac{1}{1 + \cfrac{D_B(y_B - (\gamma_B x_B/\Gamma_B)\exp(\Delta\mu_B{}^o/RT)}{D_A(y_A - (\gamma_A x_A/\Gamma_A)\exp(\Delta\mu_A{}^o/RT)}} \tag{23}$$

The step density, f, and the intermolecular spacing, λ, have cancelled out. Equation (23) can be explicitly solved for the solid composition in terms of the interfacial liquid composition and temperature.

If the compounds are similar enough to possess appreciable solid solubility, it would be a good approximation in many cases to assume that the ratio of interfacial transport coefficients, D_B/D_A, is near unity. The nonequilibrium solid composition can then be obtained from the interfacial liquid composition and temperature by using only thermodynamic equilibrium properties of the system, that is, pure component chemical potentials and the activity coefficient relationships for the two phases.

An estimate of the nonequilibrium solid composition due to a given undercooling may be obtained by applying the absolute rate theory relationship in a slightly different manner. Consider the situation depicted on the phase diagram in Figure 7. Liquid of interfacial composition, y_A, is freezing under conditions where the undercooling at the interface is ΔT degrees.

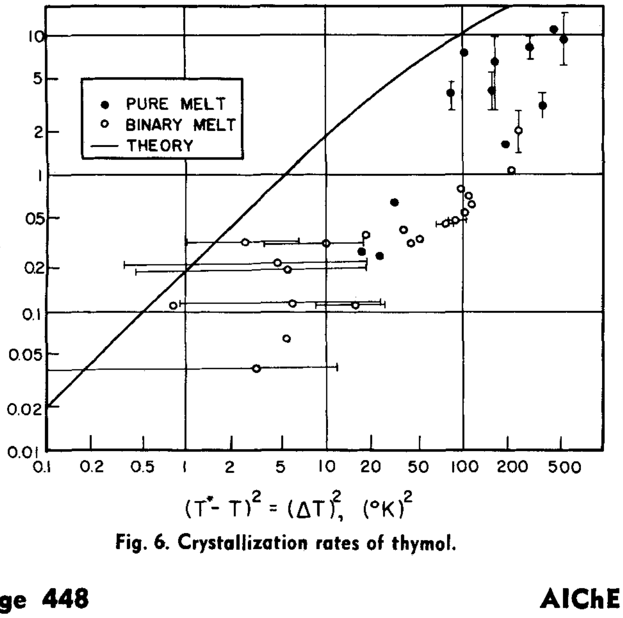

Fig. 6. Crystallization rates of thymol.

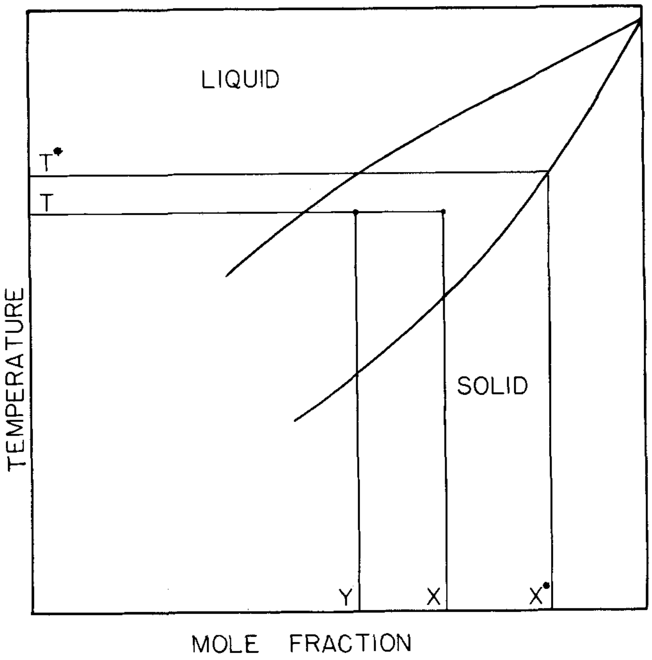

Fig. 7. Phase relationships during nonequilibrium freezing.

The ratio of the composition of A, in the solid to that of B is given by

$$x_A/x_B = \frac{D_A(y_A - (\gamma_A x_A/\Gamma_A)\exp(\Delta\mu_A{}^o/-RT)}{D_B(y_B - (\gamma_B x_B/\Gamma_B)\exp(\Delta\mu_B{}^o/-RT)} \tag{24}$$

The driving force terms may be related to the deviations of the solid composition and temperature from their equilibrium values by a Taylor series expansion about the equilibrium condition (y_A, $x_A{}^*$, T^*). Higher order terms and the small changes in the activity coefficient ratios with temperature and composition are neglected. The departure of the solid composition from its equilibrium value is then shown to be proportional to the undercooling of the liquid at the interface. Thus

$$\Delta x \equiv x_A{}^* - x_A$$

$$= \frac{x_A{}^* x_B{}^* \dfrac{\Delta H_B{}^o}{RT^2}\left[1 - \dfrac{D_A\, K_B{}^*}{D_B\, K_A{}^*}\left(\dfrac{\Delta H_A{}^o}{\Delta H_B{}^o}\right)^*\right]}{x_A{}^* + \dfrac{D_A\, K_B{}^*}{D_B\, K_A{}^*}\, x_B{}^*}\,\Delta T \tag{25}$$

where $K_i{}^*$ is the equilibrium distribution coefficient of component, i.

$$K_i{}^* = x_i{}^*/y_i{}^* = (\Gamma_i/\gamma_i)\exp(-\Delta\mu_i{}^o/RT) \tag{26}$$

An expression similar to Equation (25) can be obtained from some recent Russian work (*38*) in which kinetic equations of alloy crystallization are derived from irreversible thermodynamics; although the kinetic coefficients that are analogous to the D_i's in this work cannot be obtained from irreversible thermodynamics.

If A is the component more soluble in the solid, $K_A{}^* > 1$ and $K_B{}^* < 1$. In systems with appreciable solid solubility the interface transport coefficient ratio and the latent heat of fusion ratio probably do not differ significantly from 1.0. Under these conditions $\Delta x > 0$ and the separation achieved is less than the equilibrium value as one might intuitively expect. Whether the separation achieved under nonequilibrium conditions is greater or less than that at equilibrium is dependent upon the sign of the numerator of Equation (25). Although, as mentioned above, the separation would normally be poorer under nonequilibrium conditions, it may be that there are some cases where a separation greater than that at equilibrium could be obtained.

CONCLUSIONS

1. The microinterferometric technique used with a microscope hot stage provides a method of obtaining melt compositions very near the interface of a growing crystal. Hence, interfacial crystallization kinetics of many systems may be studied and evaluated for their effect on the design of crystallization processes for separation and purification. The technique is especially suitable for organic systems which normally crystallize relatively slowly and often form eutectic systems with little or no solid solubility.

2. The absolute rate theory expression for the crystallization of a component from the melt predicts growth rates within an order of magnitude for a wide variety of pure materials. It also correlated growth rates of salol and thymol crystals from their binary melts. The application of the absolute rate theory expression to isomorphous systems relates the composition of solid obtained under nonequilibrium conditions to the undercooling of the interfacial liquid.

ACKNOWLEDGMENT

The authors express their thanks to the National Science Foundation for its support.

NOTATION

c_p = molar heat capacity, cal./mole-°K.
D = interface transport coefficient, sq.cm./sec.
f = density of steps on surface
G = Gibbs free energy, cal./mole
h = Planck's constant, erg./sec.
H = molar enthalpy, cal./mole
k = Boltzmann's constant, erg./°K.
K = distribution coefficient
N = crystallization flux, moles/sq.cm.-sec.
r = radius, cm.
R = gas constant, cal./mole-°K.
S = molar entropy, cal./mole-°K.
T = temperature, °K.
T_i = melting point of pure i, °K.
V^j = molar volume of phase j, cc./mole
V = interface velocity, cm./sec.
x = mole fraction in solid
y = mole fraction in liquid

Greek Letters

γ = activity coefficient in solid phase
Γ = activity coefficient in liquid phase
η = viscosity, poises
κ = transmission coefficient
λ = distance interface advances with the addition of a monomolecular layer, cm.
μ = chemical potential, cal./mole
ρ = molar density, moles/cc.
σ = interfacial free energy, cal./sq.cm.

Superscripts

$*$ = equilibrium value
$\neq$ = activated state property
o = standard state property
f = forward direction
h = hole formation process
j = jumping process
l = liquid
r = reverse direction
s = solid

Subscripts

A, B, i = species A, B, or i
v = viscous flow property

LITERATURE CITED

1. Powers, J. E., *Hydrocarbon Process. Petrol. Refiner* **45**, 97 (1966).
2. Zief, M. and W. R. Wilcox, ed., "Fractional Solidification," Marcel Dekker, Inc., New York (1967).
3. Van Hook, A., "Crystallization," Rheinhold, New York (1963).
4. Chalmers, B., "Principles of Solidification", John Wiley, New York (1964).
5. Cahn, J., W. Hillig, and G. Sears, *Acta. Met.*, **12**, 1421 (1964).
6. ———, *ibid.*, 8, 554 (1960).
7. Jackson, K., "Growth and Perfection of Crystals," R. H. Doremus, B. W. Roberts, and David Turnbull, ed., John Wiley, New York (1958).
8. Hillig, W. B., and D. Turnbull, *J. Chem. Phys.*, **12**, 914 (1956).
9. Mullin, J. W., "Crystallization," Butterworths, London (1961).
10. McCabe, W., and J. Smith, "Unit operations of Chemical Engineering," McGraw-Hill, New York (1956).
11. Glasstone, S., K. Laidler, and H. Eyring, "Theory of Rate Processes," McGraw-Hill, New York (1941).
12. Clifton, D., Ph.D. thesis, Univer. of Utah, Salt Lake City (1957).
13. Frank, F. C., *Discussions Faraday Soc.*, **5**, 48 (1948).
14. Burton, W., N. Cabrera, and F. C. Frank, *Phil. Trans. Roy. Soc. London, Ser. A*, **198**, 205 (1949).
15. Magill, J. H., and D. J. Plazek, *Nature*, **209**, 5018 (1966).
16. Whitaker, S., and R. L. Pigford, *Ind. Eng. Chem.*, **50**, 1026 (1958).
17. Bondi, A., *J. Chem. Phys.*, **14**, 591 (1946).
18. Turnbull, D., *Sci. Amer.*, **212**, 38 (1965).
19. Hirschfielder, J., C. Curtis, and R. B. Bird, "Molecular Theory of Gases and Liquids," John Wiley, New York (1954).
20. Berg, W., *Proc. Roy. Soc. (London) Ser. A*, **164**, 79 (1938).
21. Bunn, C., *Discussions Faraday Soc.*, **5**, (1949).
22. Humphreys-Owen, S., *Proc. Roy. Soc. (London) Ser. A*, **197**, 218 (1948).
23. Nishijima, Y., and G. Oster, *J. Polymer Sci.*, **19**, 337 (1956).
24. Secor, R., *AIChE J.*, **11**, 452 (1965).
25. Kirwan, D. J., Ph.D. thesis, Univ. Delaware, Newark (1967).
26. Timmermanns, J., "Physico-Chemical Constants of Binary Systems in Concentrated Solutions," Vol. 2, p. 1169, Interscience, New York (1959).
27. Jantsch, O., *Z. Krist.*, **108**, 185 (1956).
28. Micus, G., and U. Trollenier, *Z. Elektrochem.*, **59**, 412 (1955).
29. Turnbull, D., "Solid State Phys.," Vol. 3, p. 225 Academic Press, New York (1958).
30. Bondi, A., in "Rheology," Vol. I., F. Eirich, ed., Academic Press, New York (1956).
31. Hudson, J., and G. Sears, *J. Chem. Phys.*, **35**, 1509 (1961).
32. Kramer, J., and W. Tiller, *ibid.*, **42**, 257 (1965).
33. Walker, J., see reference **4**, p. 114.
34. Pollatschek, H., *Z. Physik. Chem.*, **142A**, 289 (1929).
35. Newmann, K., and G. Micus, *ibid.*, **2**, 25 (1954).
36. Votava, E., S. Amelinckx, and W. Dekeyser, *Naturwiss.*, **39**, 547 (1952).
37. *Ibid.*, **40**, 143, 290 (1953).
38. Sirota, N. N., F. K. Gorskii, and V. M. Varikash, ed., "Crystallization Processes," The Consultants Bureau, New York (1966).

Manuscript received September 28, 1967; revision received March 8, 1968; paper accepted March 25, 1968. Paper presented at AIChE Tampa meeting.